ACS APPLIED MATERIALS & INTERFACES

Research Article

Cite This: ACS Appl. Mater. Interfaces 2019, 11, 10237−10243

www.acsami.org

Experimental Investigation on Vertically Oriented Graphene Grown in a Plasma-Enhanced Chemical Vapor Deposition Process

Yifei Ma,[†] Wei Jiang,[‡] Jiemin Han,[†] Zhaomin Tong,[†] Mei Wang,*[,†] Jonghwan Suhr,[§] Xuyuan Chen,[†,⊥] Liantuan Xiao,[†] Suotang Jia,[†] and Heeyeop Chae*[,‡,∥]

[†]State Key Laboratory of Quantum Optics and Quantum Optics Devices, Institute of Laser Spectroscopy, Collaborative Innovation Center of Extreme Optics, Shanxi University, Taiyuan, Shanxi 030006, People's Republic of China

[‡]School of Chemical Engineering, [§]Department of Polymer Science and Engineering, Department of Energy Science, Department of Mechanical Engineering, and [∥]SKKU Advanced Institute of Nanotechnology (SAINT), Sungkyunkwan University (SKKU), Suwon 16419, Republic of Korea

[⊥]Faculty of Technology, Natural Sciences and Maritime Sciences, Department of Microsystems, University of Southeast Norway, Borre N-3184, Norway

Supporting Information

ABSTRACT: Vertically oriented graphene (VG) with three-dimensional architecture has been proved to exhibit unique properties, and its particular morphology has been realized by researchers to be crucial for its performance in practical applications. In this study, we investigated the morphology evolution of VG films synthesized by the plasma-enhanced chemical vapor deposition process, including porous graphene film, graphene wall, and graphene forest. This study reveals that the morphology of VG is controlled by a combination of the deposition and etching effects and tailored by the growth conditions, such as plasma source power and growth time and temperature. The plasma source power relates to the number of branches of VG, and the growth temperature relates to the thickness of each VG flake, whereas the growth time determines the height of VG. Finally, the electrochemical properties of VG films along with morphology evolution are investigated by fabricating as VG-based supercapacitor electrodes.

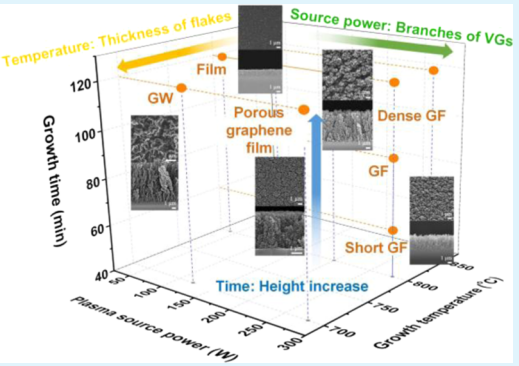

KEYWORDS: *vertically oriented graphene, PECVD, graphene wall, graphene forest, porous graphene film, morphology formation mechanism*

INTRODUCTION

Vertically oriented graphene (VG), compared with conventional two-dimensional (2D) graphene sheets, possesses advantageous characteristics, including exposed sharp edges, nonstacking morphology, and a high surface-to-volume ratio.[1] VG has been predominantly achieved by the plasma-enhanced chemical vapor deposition (PECVD) process with few exceptions where sputtering techniques have been used[1] and has been widely studied as three-dimensional (3D) carbon-based versatile building blocks for various applications, such as supercapacitors,[2−4] field emission devices,[5] sensors,[6,7] etc. It is worth noting that the performances of VG in these applications are related to its electrical conductivity and, more importantly, its 3D morphology,[8] including the alignment of vertical graphene sheets, porosity of VG films, stacking of graphene sheets in horizontal and perpendicular directions, thickness of vertically aligned VG layers, and so on.

The reported VGs grown by the PECVD so far are "graphene wall" (GW)[8−13] and "graphene forest" (GF),[14] where the wall flakes or the trees with piled flakes are the configuration elements. Research studies on the GWs and GFs have been carried out by controlling the height, density, and alignment of the configuration elements. More importantly, the emergence of GF subverts the structure stereotype of VG, bringing the possibility to synthesize VG with more diversified morphologies. However, the key synthetic factors affecting the morphology of VGs have not been clearly understood and the morphology control of VGs has not been achieved. Accordingly, it is critical to identify a set of synthetic factors affecting the morphology of VGs and to achieve the controllable structure of VGs.

In this study, we investigate the growth-condition-dependent structure of VGs. The morphology of VGs' structure has been analyzed according to plasma source power and growth time and temperature to explore the PECVD process conditions for growing VGs with a controllable morphology. Then, the electrochemical performance of VGs according to the morphology change was characterized by fabricating the

Received: January 15, 2019
Accepted: February 22, 2019
Published: February 22, 2019

DOI: 10.1021/acsami.9b00896
ACS Appl. Mater. Interfaces 2019, 11, 10237−10243

supercapacitors with VG electrodes. We confidently believe that this study has momentous guiding significance for comprehensively understanding and exploitation of diversiform VGs and for growing VGs with controllable structure morphology, thereby achieving the customization of graphene nanostructures and expediting the utilization of VGs for further applications.

EXPERIMENTAL SECTION

Preparation of VGs. The synthesis method of VGs by the PECVD technique has been reported in previous studies.[14,15] In brief, a 5 × 5 cm^2 quartz plate was used as the substrate that was placed in the heating zone of a tube-type inductive coupled PECVD system as shown in Figure S1. Before the graphene growth, the PECVD chamber was cleaned with hydrogen gas at a flow rate of 8 sccm and a temperature of 800 °C for 5 min to remove surface oxygen on the quartz substrate. Plasma was then generated with a radio frequency source power of 200 W and worked subsequently for 3 min to further remove contaminants on the quartz substrate. Then, VG was grown by introducing C_2H_2 and H_2 at the flow rates of 3 and 1 sccm, respectively. The pressure inside the chamber was around 60 mTorr. The VGs were obtained at different synthetic conditions, such as plasma source power and growth time and temperature, which were varied to research their effects on the morphology of VGs. The experimental schemes are listed in Table 1 for the investigation of the plasma source-power-dependent growth, the time-dependent growth, and the temperature-dependent growth, respectively.

Table 1. Experimental Schemes of Growth Conditions

investigation schemes (#)	plasma source power (W)	growth time (min)	growth temperature (°C)
#1 for the power-dependent growth	40−280	120	800
#2 for the time-dependent growth	280	10−120	800
#3 for the temperature-dependent growth	280	120	700−800
	120	120	700−800

Fabrication of VG-Based Supercapacitors. Poly(vinyl alcohol) (PVA) was utilized to prepare a polymer electrolyte. PVA (98−99% hydrolyzed, medium molecular weight, Alfa Aesar) powder was dissolved in deionized water (2 g PVA/20 mL H_2O) and heated under stirring to around 90 °C in an oil bath until the solution became clear. Then, 1.6 g of concentrated phosphoric acid was added to the solution with thorough stirring.

Three milliliters of the as-prepared PVA solution was directly spun-coated onto the surface of VG on a quartz plate and dried in air. The PVA/VG film was then carefully peeled off from the quartz substrate. The PVA surface is quite sticky and therefore two pieces of the PVA/VG films can stack together easily to form a VG/PVA/PVA/VG structure. Two copper plates were applied to pack the stacked GF/PVA/PVA/GF layers and worked as the current collectors.

Characterization of Materials. The surface and cross-sectional morphologies of VGs on quartz substrates were examined with field emission scanning electron microscopy (FE-SEM, JEOL, JSM7500F). Carbon bonding structure of VGs was analyzed by Raman spectroscopy (Renishaw, RM-1000 Invia) with a wavelength of 532 nm. High-resolution transmission electron microscopy (HRTEM, JEM-2100F JEOL) images were also taken to show the structure of the graphene flakes. The sheet resistance was measured using the four-point probe method (Keithley 2420I−V) by selecting 10 random points on the surface of each sample. The detector with linearly arranged four probes was perpendicularly contacted with the surface of sample at room temperature without additional treatment. Electrochemical properties of the supercapacitor were analyzed with a electrochemical workstation (Biologic, VSP-300).

RESULTS AND DISCUSSION

Effect of Plasma Source Power. Compared with the conventional thermal CVD method for growing the single/few-layer 2D graphene films, the PECVD growth can realize the 3D pileup of carbon atoms owing to the sheath effect of the plasma.[16] Thus, during the process of growing VGs by PECVD, the most direct and controllable parameter is the source power of inductively coupled plasma. Herein, a series of VGs are fabricated at different plasma source power, whereas the growth time and temperature are fixed at 120 min and 800 °C, respectively. The evolution of morphology depending on the plasma source power is illustrated by top and cross-sectional SEM images in Figure 1a,b. At the plasma source

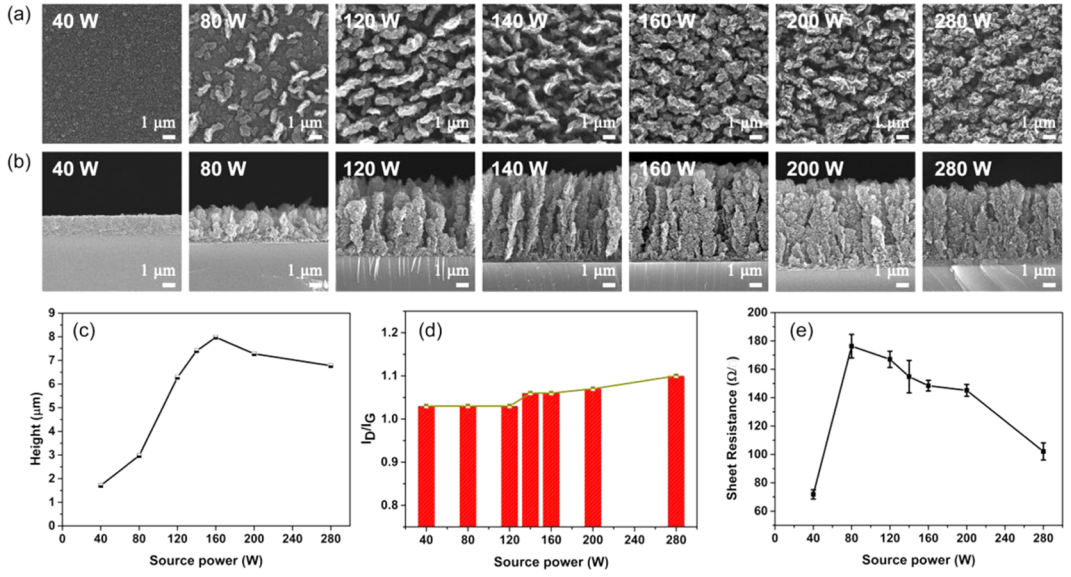

Figure 1. Dependence of VG morphologies and properties on plasma source power. Top-view (a) and cross-sectional (b) SEM images of VGs, height variation of VGs (c), the intensity ratio of D to G peaks (d), and the sheet resistance of VGs (e) grown at different plasma source powers.

DOI: 10.1021/acsami.9b00896
ACS Appl. Mater. Interfaces 2019, 11, 10237−10243

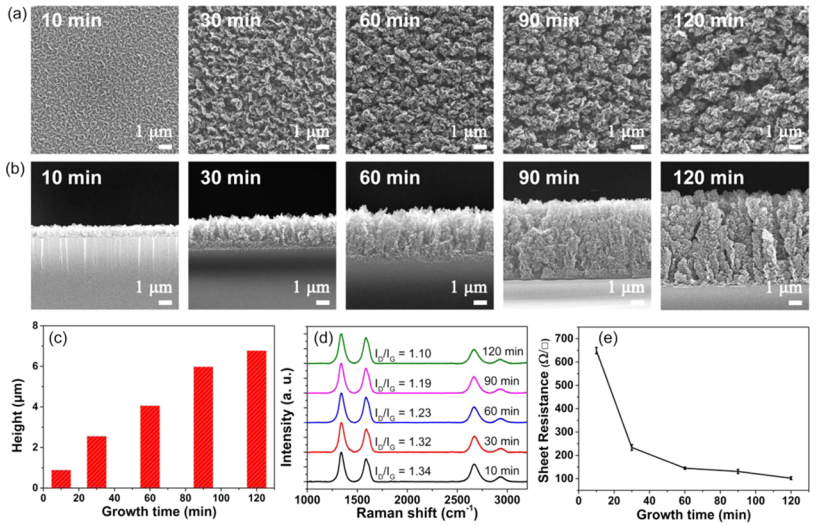

Figure 2. Dependence of VG morphologies and properties on growth time. Top-view (a) and cross-sectional (b) SEM images of VGs, height variation of VGs (c), the intensity ratio of D to G peaks (d), and the sheet resistance of VGs (e) grown at different growth times.

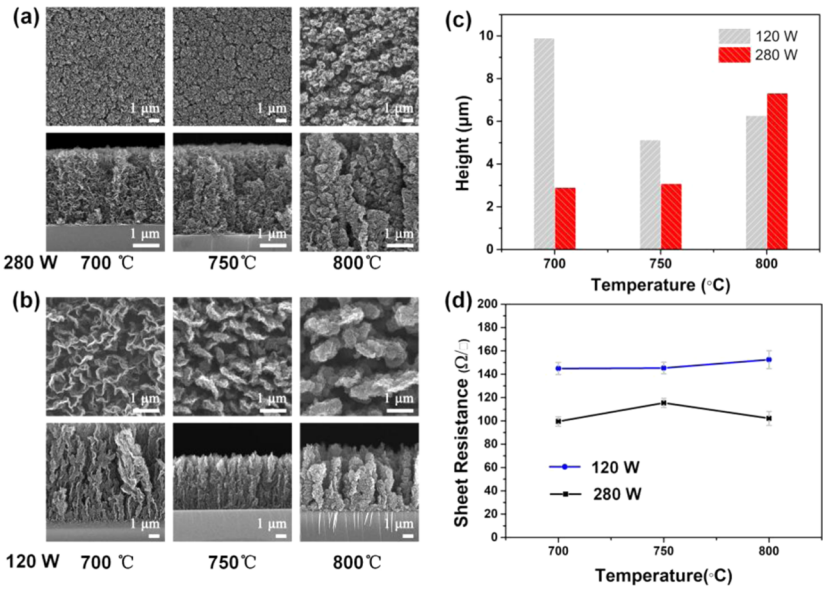

Figure 3. Dependence of VG morphologies and properties on growth temperature. Top-view and cross-sectional SEM images of VGs at different growth temperatures with the plasma source powers of 280 W (a) and 120 W (b). Height of VGs synthesized at different temperatures and plasma source powers of 120 and 280 W (c). The sheet resistance of VGs synthesized at different temperatures and the plasma source powers of 120 and 280 W (d).

power of 40 W, not GF, a microscale flat film with bare VG sheets is obtained on the substrate (Figure 1b). However, with the increase of the plasma source power, unlike thin nanosheet in GW, thick vertically standing flakes start to appear at the plasma source power of 80 W. With continuous increase of the source power, the vertically standing flakes grow larger and bushier, which look like "trees", forming the GFs. Accordingly, the height of GF also increases to a saturated value of 8.0 μm at 160 W, as shown in Figure 1c.

Raman spectrum is an important detective method widely used to reveal the quality of graphene and to estimate the number of graphene layers.[17] Unluckily, since each graphene nanosheet in VG is composed of 10−20 layers of graphene (Figure S2),[14,18,19] rather than monolayer or few layers, it is hard to estimate the layer numbers of graphene according to the intensity ratios of 2D and G peaks (I_{2D}/I_G) from Raman spectra. Nevertheless, peak intensity ratios of D and G peaks (I_D/I_G) are applicable to characterize the level of disorder and defects in graphene.[20] The Raman spectra of VGs grown at different plasma source powers and the I_D/I_G are shown in Figures 1d and S3, respectively. As the plasma source power increases, a very slight increment of I_D/I_G is observed. Hence, we can conclude that the increase of plasma source power will not significantly affect the level of disorder and defects in VGs.

Resistivity is another important property of graphene, which directly affects the performance of graphene-based devices. Because of the unique 3D morphology of VGs, the sheet resistance is related to not only the quality of GF but also its nanostructures. As shown in Figure 2d, the sheet resistance of VGs decreases with the increase of plasma source power with the exception of the flat graphene film grown at 40 W. According to the SEM images in Figure 1, the graphene "tree"

DOI: 10.1021/acsami.9b00896
ACS Appl. Mater. Interfaces 2019, 11, 10237−10243

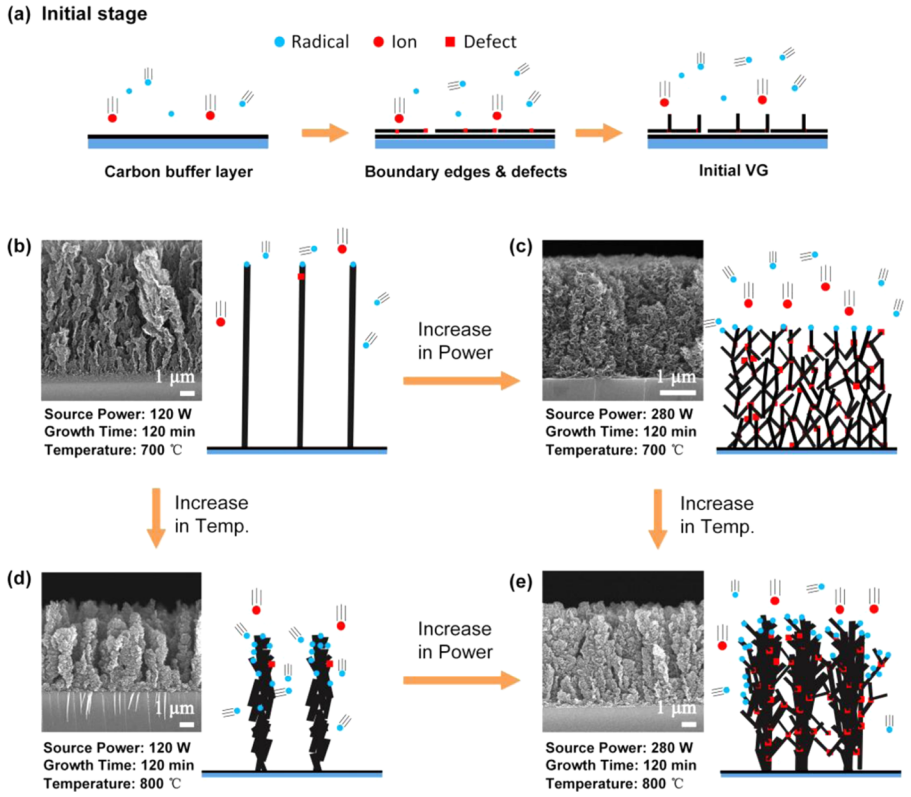

Figure 4. Schematic diagrams of the growth mechanism of VGs under different growth conditions: (a) initial stage; (b) VG grown at a relatively low temperature and low plasma source power; (c) increase of plasma source power; (d) increase of temperature; and (e) GF grown at a relatively high temperature and high plasma source power.

is barely observed on the film grown at 40 W, so the film cannot be treated as GF or even VG. Obviously, the compact in-plane structure of the graphene film grown at 40 W will have a lower sheet resistance compared to that of other vertically oriented structures. As the plasma source power further increases, the GF becomes denser and a better connection between graphene "trees" is formed; thus, the in-plane electron transfer becomes easier and faster, resulting in an abatement of the sheet resistance.

Effect of Growth Time. The dense GFs are representative to present the morphology evolution of VG depending on time. Hence, GFs grown at 280 W and 800 °C are fabricated with different growth times from 10 to 120 min to investigate the influence of time on morphology. As shown in Figure 2a,b, thin GF films are obtained on the substrate with short nanoscale graphene trees when the growth time is less than 30 min, looking like the "saplings" of the GF. However, when the growth time increases to 60 min and even longer, the graphene trees continuously grow higher in a nearly linear increment, as shown in Figure 2c. In spite of the height, the corresponding cross-sectional SEM images in Figure 2b clearly illustrate that all VGs grown with different times have the structure of GF so that the morphology of VG is not obviously affected by the growth time. In the Raman spectra of Figures 2d and S4, the I_D/I_G decreases with increasing growth time, indicating the reduction in defects. In addition, as GF becomes thicker and larger, the I_{2D}/I_G also decreases with increasing growth time, which indicates that the number of graphene layers in GF increases with the longer growth time. Moreover, as the growth time increases from 10 to 60 min, the GF grows denser and taller, forming a better connection between each graphene tree. Thus, owing to the fewer defects and the better connection, the sheet resistance decreases rapidly when the growth time increases from 10 to 60 min, and then the resistance decreases gradually because of fewer defects grown for more than 60 min, as illustrated in Figure 2e.

Effect of Growth Temperature. The growth temperature is also a crucial factor that may greatly influence the morphology of VG, which may work together with plasma source powers. Hence, VGs are synthesized at 700, 750, and 800 °C with the growth time of 120 min at the plasma source powers of 120 and 280 W, respectively. First, at 280 W, as shown in Figure 3a, significant morphology difference of VGs is observed when the growth temperature decreases: the distance between each graphene tree greatly reduces, and the size of each graphene tree becomes larger. The graphene flakes in graphene trees are connected with each other (Figure S5), so a more continuous porous film is formed on the substrate at the lower growth temperature. Meanwhile, the height of the VG film also decreases along with the decrease of growth temperature (Figure 3c).

Second, as shown in Figure 3b, the key factors to synthesize GW can be inferred to be low temperature and plasma source power. As the growth temperature decreases, the graphene trees consecutively become thinner. Finally, a representative GW is obtained at the growth temperature of 700 °C. Raman spectra of the as-prepared VGs are illustrated in Figure S6. The intensity ratios of D to G peaks at 280 and 120 W both increase along with the decrease of temperature, which indicates that more defects are generated at a lower temperature. In addition, the sheet resistance almost keeps stable within an acceptable fluctuation (Figure 3d).

DOI: 10.1021/acsami.9b00896
ACS Appl. Mater. Interfaces 2019, 11, 10237−10243

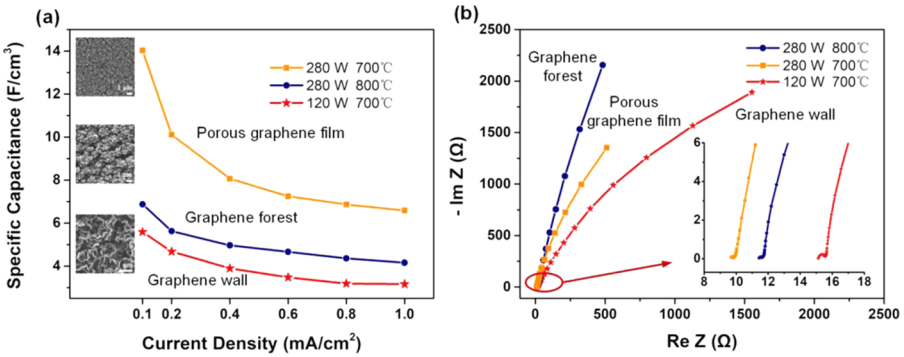

Figure 5. (a) Specific capacitances of supercapacitors based on the porous graphene film, GF, and GW as functions of current densities. (b) Nyquist plots of supercapacitors based on the porous graphene film, GF, and GW.

Growth Mechanism. In the PECVD process, hydrocarbon gases are ionized and the generated radicals and ions exhibit deposition effect and etching effect, respectively.[21,22] As reported in previous research studies,[22−24] the etching by ion bombardment will induce defects that may serve as the active site for growth, whereas the radicals (the primary source of C_xH_y radicals) will promote the growth of VGs. Although it is hard to determine the role of each ion and radical using the presently available experimental techniques,[22,25] inferred from the morphology change of VGs at different conditions, the overall growth can be explained by the balance of etching and deposition effects, as summarized in Figure 4. We conclude that the growth of VGs in the PECVD process is synergistically affected by plasma source power, growth temperature, and growth time. Based on the morphology of VGs at different growth conditions, we speculate the mechanism of the morphology formation in detail as follows.

Initially, the carbon buffer layers first grow on the surface of the substrate in parallel to reduce the lattice mismatch between the substrate and graphene, as shown in Figure 4a. Then, graphene begins to grow vertically due to three reasons:[13,24] (1) the simultaneous growth of graphene and amorphous carbon leads to discontinuity of horizontal graphene growth; (2) strain energy in the edges and defects in initial graphene; and (3) sheath effect accelerates the energetic ions to affect the surface of substrate, resulting in defects that help graphene grow vertically. Here, the plasma source power will determine the density of VG. This is because when the plasma source power increases, the density of ions increases, resulting in increased defects for vertical growth. On the other hand, if the plasma source power is too low (e.g., 40 W), no VG is obtained, as shown in Figure 1a.

The morphology of VGs is subject to the growth condition after initial stage. Under low plasma source power and low growth temperature, as shown in Figure 4b, the densities of ions and radicals are low with low reaction activities. Then, radicals are prone to bond at the edge of graphene flakes where the required activation energy is relatively low, resulting in thin in-plane growth of "wall-like" graphene. When the plasma source power is increased, the densities of ions and radicals increase simultaneously.[26,27] The increased ion bombardment will create abundant defects for radicals to be deposited, thereby bifurcating the graphene tree and forming branches.[24] As a result, the porous graphene is obtained (Figure 4c). As the surface temperature increases, the surface reaction rate is enhanced. The radicals get enough energy to be deposited not only at the edge of graphene flakes but also on the surface. Thus, the graphene flakes become much thicker (Figure 4d) than those grown at low temperature. If the temperature and plasma source power are both increased, plenty of ions and radicals with high activities exist in the chamber. Accordingly, thick graphene flakes with many branches can be obtained on the substrate, as shown in Figure 4e.

It is worth noting that the growth rate (VG height/growth time) results from the balance of etching and deposition effects. On the one hand, at 700 °C and 120 W, though the radical density and ion energy are low at the low plasma source power, ions can be chemically adsorbed to the substrate,[28] thereby not only creating defects (radical sites) for growth to occur via radical grafting but also depositing themselves. As a result, the deposition rate and the VG height are relatively high (Figure 3c). On the other hand, a high temperature and a high plasma source power will increase the radical density and ions energy. Ions will also cause a strong etching effect, thus decreasing the deposition rate and VG height when the ions are too energetic. Therefore, the height of VG is decreased and defects are increased when the plasma power is higher than 160 W at 800 °C (Figure 1a).

Furthermore, growth time does not determine the morphology of VGs but influences the height of the vertical flakes in VGs because the activities and densities of ions and radicals do not change during the growth process. Thus, by controlling the growth time, the VGs with different heights can be obtained.

Electrochemical Properties. To comprehensively understand the morphologies and properties of VGs, the electrochemical properties of VGs with different morphologies have been investigated. Accordingly, supercapacitors were fabricated based on three typical types of VG electrodes: GWs with thin vertical graphene sheets that were fabricated at 120 W, 700 °C for 2 h; GFs with stacked graphene flakes that were fabricated at 280 W, 800 °C for 2 h; and porous graphene films with porous structures that were fabricated at 280 W, 700 °C for 2 h.

Galvanostatic charge/discharge and cyclic voltammetry (CV) test were performed as shown in Figure S7. The symmetric triangular slopes of galvanostatic charge/discharge curves and the rectangular shape of CV plots indicate the instantaneous formation of electric double-layer and the desirable ion diffusion within the electrodes. Then, the specific capacitances at various current densities are plotted in Figure 5a. The porous graphene film-based supercapacitor exhibited the highest volumetric capacitance that reaches 14.03 F/cm^3 (at the current density of 0.1 mA/cm^2), whereas the GW-based

DOI: 10.1021/acsami.9b00896
ACS Appl. Mater. Interfaces 2019, 11, 10237−10243

supercapacitor only provides a volumetric capacitance of 5.59 F/cm^3 (at a current density of 0.1 mA/cm^2). It is reasonable that porous graphene film can provide a higher specific capacitance than the GF and GW due to the denser configuration of graphene flakes.

The electrochemical impedance spectroscopy was characterized as shown in Nyquist plots (Figure 5b). Attributed to the continuous porous structure of the electrode material, the equivalent series resistance of the porous graphene film-based supercapacitor is slightly lower than that of GF. In addition, the porous graphene film and GW are fabricated at a relatively low temperature (700 °C), in which defects are introduced and internal resistances are increased. As a result, the supercapacitors based on the porous graphene film and GW show a nonideal slope at the low-frequency region. Furthermore, the Bode plots are illustrated in Figure S8. At the phase angle of −45°, the resistance and reactance of the supercapacitors have equal magnitudes and therefore the frequency at this point is used for comparison.[3] Benefiting from the wall-like structure, the electrolyte ions have a shorter diffusion pathway, thereby easily accessing the surface of the GW. Hence, the GW-based supercapacitor reaches the highest frequency at the phase angle of −45°.

CONCLUSIONS

In this study, the morphology evolution of VGs in the PECVD process is thoroughly investigated by varying the synthetic factors such as plasma source power, growth time, and temperature. We conclude that the morphology of VGs is strongly dependent on the synergistic effect of the deposition and etching effects, resulting from the plasma source power and growth temperature in the PECVD process. The growth time does not determine the morphology but the final film thickness of VGs. At last, the porous graphene film-based supercapacitor shows the highest specific capacitance, whereas the GW exhibits the best frequency response, derived from their morphological properties. We strongly believe that this work has a significant guiding importance in terms of controllable synthesis of VGs and morphology optimization of VGs for the target applications.

ASSOCIATED CONTENT

Supporting Information

The Supporting Information is available free of charge on the ACS Publications website at DOI: 10.1021/acsami.9b00896.

Setup image of the reactor (Figure S1), TEM images of GW, GF, and porous graphene (Figure S2), Raman spectra of VGs fabricated at different plasma source power (Figure S3) and at different temperatures (Figure S6), intensity ratios of D to G peak and 2D to G peak of VGs at different growth times (Figure S4), SEM images of VGs at different growth temperatures (Figure S5), galvanostatic charge/discharge and cyclic voltammetry (Figure S7) and Bode plots (Figure S8) of VGs-based supercapacitor (PDF)

AUTHOR INFORMATION

Corresponding Authors

*E-mail: wangmei@sxu.edu.cn (M.W.).
*E-mail: hchae@skku.edu (H.C.).

ORCID

Heeyeop Chae: 0000-0002-6380-0414

Notes

The authors declare no competing financial interest.

ACKNOWLEDGMENTS

This research was supported by the National Key R&D Program of China (Grant No. 2017YFA0304203), the National Natural Science Foundation of China (Grants Nos. 21805174 and 11434007), the 111 Project (Grant No. D18001), the Shanxi Province 100-Plan Talent Program, the Changjiang Scholars and Innovative Research Team in University of Ministry of Education of China (Grant No. IRT_17R70), the Key Research and Development Program of Shanxi Province for International Cooperation (201803D421082), the Applied Basic Research Project of Shanxi Province (201801D221100), the Fund for Shanxi "1331 Project" Key Subjects Construction, the National Research Foundation of Korea (NRF) grant funded by the Korea government (MSIT) (2018R1A2A3074950), and the Korea Institute of Energy Technology Evaluation and Planning (KETEP) grant funded by the Korea government Ministry of Trade, Industry and Energy (20172010104830).

REFERENCES

(1) Bo, Z.; Yang, Y.; Chen, J.; Yu, K.; Yan, J.; Cen, K. Plasma-Enhanced Chemical Vapor Deposition Synthesis of Vertically Oriented Graphene Nanosheets. *Nanoscale* **2013**, *5*, 5180−5204.

(2) Shen, H.; Li, H.; Li, M.; Li, C.; Qian, L.; Su, L.; Yang, B. High-Performance Aqueous Symmetric Supercapacitor Based on Polyaniline/Vertical Graphene/Ti Multilayer Electrodes. *Electrochim. Acta* **2018**, *283*, 410−418.

(3) Sheng, K.; Sun, Y.; Li, C.; Yuan, W.; Shi, G. Ultrahigh-Rate Supercapacitors Based on Eletrochemically Reduced Graphene Oxide for AC Line-Filtering. *Sci. Rep.* **2012**, *2*, No. 247.

(4) Zhang, Y.; Zou, Q.; Hsu, H. S.; Raina, S.; Xu, Y.; Kang, J. B.; Chen, J.; Deng, S.; Xu, N.; Kang, W. P. Morphology Effect of Vertical Graphene on the High Performance of Supercapacitor Electrode. *ACS Appl. Mater. Interfaces* **2016**, *8*, 7363−7369.

(5) Deng, J.-H.; Liu, R.-N.; Zhang, Y.; Zhu, W.-X.; Han, A. L.; Cheng, G.-A. Highly Improved Field Emission from Vertical Graphene−Carbon Nanotube Composites. *J. Alloys Compd.* **2017**, *723*, 75−83.

(6) Mao, S.; Yu, K.; Chang, J.; Steeber, D. A.; Ocola, L. E.; Chen, J. Direct Growth of Vertically-Oriented Graphene for Field-Effect Transistor Biosensor. *Sci. Rep.* **2013**, *3*, No. 1696.

(7) Huang, S.; He, G.; Yang, C.; Wu, J.; Guo, C.; Hang, T.; Li, B.; Yang, C.; Liu, D.; Chen, H.-J.; Wu, Q.; Gui, X.; Deng, S.; Zhang, Y.; Liu, F.; Xie, X. Stretchable Strain Vector Sensor Based on Parallelly Aligned Vertical Graphene. *ACS Appl. Mater. Interfaces* **2018**, *11*, 1294−1302.

(8) Premathilake, D.; Outlaw, R. A.; Parler, S. G.; Butler, S. M.; Miller, J. R. Electric Double Layer Capacitors for AC Filtering Made from Vertically Oriented Graphene Nanosheets on Aluminum. *Carbon* **2017**, *111*, 231−237.

(9) Yang, H.; Yang, J.; Bo, Z.; Zhang, S.; Yan, J.; Cen, K. Edge Effects in Vertically-Oriented Graphene Based Electric Double-Layer Capacitors. *J. Power Sources* **2016**, *324*, 309−316.

(10) Ghosh, S.; Ganesan, K.; Polaki, S. R.; Ravindran, T. R.; Krishna, N. G.; Kamruddin, M.; Tyagi, A. K. Evolution and Defect Analysis of Vertical Graphene Nanosheets. *J. Raman Spectrosc.* **2014**, *45*, 642−649.

(11) Hsu, C.-C.; Bagley, J. D.; Teague, M. L.; Tseng, W.-S.; Yang, K. L.; Zhang, Y.; Li, Y.; Li, Y.; Tour, J. M.; Yeh, N. C. High-Yield Single-Step Catalytic Growth of Graphene Nanostripes by Plasma Enhanced Chemical Vapor Deposition. *Carbon* **2018**, *129*, 527−536.

(12) Yue, Z.; Levchenko, I.; Kumar, S.; Seo, D.; Wang, X.; Dou, S.; Ostrikov, K. Large Networks of Vertical Multi-Layer Graphenes with

DOI: 10.1021/acsami.9b00896
ACS Appl. Mater. Interfaces 2019, 11, 10237−10243

Morphology-Tunable Magnetoresistance. *Nanoscale* **2013**, *5*, 9283−9288.
(13) Ma, Y.; Jang, H.; Kim, S.; Pang, C.; Chae, H. Copper-Assisted Direct Growth of Vertical Graphene Nanosheets on Glass Substrates by Low-Temperature Plasma-Enhanced Chemical Vapour Deposition Process. *Nanoscale Res. Lett.* **2015**, *10*, No. 308.
(14) Ma, Y.; Wang, M.; Kim, N.; Suhr, J.; Chae, H. A Flexible Supercapacitor Based on Vertically Oriented 'Graphene Forest' Electrodes. *J. Mater. Chem. A* **2015**, *3*, 21875−21881.
(15) Wang, M.; Ma, Y. Nitrogen-Doped Graphene Forests as Electrodes for High-Performance Wearable Supercapacitors. *Electrochim. Acta* **2017**, *250*, 320−326.
(16) Jiang, L.; Yang, T.; Liu, F.; Dong, J.; Yao, Z.; Shen, C.; Deng, S.; Xu, N.; Liu, Y.; Gao, H. J. Controlled Synthesis of Large-Scale, Uniform, Vertically Standing Graphene for High-Performance Field Emitters. *Adv. Mater.* **2013**, *25*, 250−255.
(17) Ferrari, A. C.; Basko, D. M. Raman Spectroscopy as a Versatile Tool for Studying the Properties of Graphene. *Nat. Nanotechnol.* **2013**, *8*, 235−246.
(18) Cai, M. Z.; Outlaw, R. A.; Butler, S. M.; Miller, J. R. A High Density of Vertically-Oriented Graphenes for Use in Electric Double Layer Capacitors. *Carbon* **2012**, *50*, 5481−5488.
(19) Quinlan, R. A.; Cai, M. Z.; Outlaw, R. A.; Butler, S. M.; Miller, J. R.; Mansour, A. N. Investigation of Defects Generated in Vertically Oriented Graphene. *Carbon* **2013**, *64*, 92−100.
(20) Cançado, L. G.; Jorio, A.; Ferreira, E. H. M.; Stavale, F.; Achete, C. A.; Capaz, R. B.; Moutinho, M. V. O.; Lombardo, A.; Kulmala, T. S.; Ferrari, A. C. Quantifying Defects in Graphene via Raman Spectroscopy at Different Excitation Energies. *Nano Lett.* **2011**, *11*, 3190−3196.
(21) Terasawa, T.; Saiki, K. Growth of Graphene on Cu by Plasma Enhanced Chemical Vapor Deposition. *Carbon* **2012**, *50*, 869−874.
(22) Mironovich, K. V.; Itkis, D. M.; Semenenko, D. A.; Dagesian, S. A.; Yashina, L. V.; Kataev, E. Y.; Mankelevich, Y. A.; Suetin, N. V.; Krivchenko, V. A. Tailoring of the Carbon Nanowall Microstructure by Sharp Variation of Plasma Radical Composition. *Phys. Chem. Chem. Phys.* **2014**, *16*, 25621−25627.
(23) Baranov, O.; Levchenko, I.; Xu, S.; Lim, J. W. M.; Cvelbar, U.; Bazaka, K. Formation of Vertically Oriented Graphenes: What Are the Key Drivers of Growth? *2D Mater.* **2018**, *5*, No. 044002.
(24) Zhang, L. X.; Sun, Z.; Qi, J. L.; Shi, J. M.; Hao, T. D.; Feng, J. C. Understanding the Growth Mechanism of Vertically Aligned Graphene and Control of Its Wettability. *Carbon* **2016**, *103*, 339−345.
(25) Qi, Y.; Deng, B.; Guo, X.; Chen, S.; Gao, J.; Li, T.; Dou, Z.; Ci, H.; Sun, J.; Chen, Z.; Wang, R.; Cui, L.; Chen, X.; Chen, K.; Wang, H.; Wang, S.; Gao, P.; Rummeli, M. H.; Peng, H.; Zhang, Y.; Liu, Z. Switching Vertical to Horizontal Graphene Growth Using Faraday Cage-Assisted PECVD Approach for High-Performance Transparent Heating Device. *Adv. Mater.* **2018**, *30*, No. 1704839.
(26) Piejak, R. B.; Godyak, V. A.; Alexandrovich, B. M. A Simple Analysis of an Inductive RF Discharge. *Plasma Sources Sci. Technol.* **1992**, *1*, 179.
(27) Ma, Y.; Kim, D.; Jang, H.; Cho, S. M.; Chae, H. Characterization of Low Temperature Graphene Synthesis in Inductively Coupled Plasma Chemical Vapor Deposition Process with Optical Emission Spectroscopy. *J. Nanosci. Nanotechnol.* **2014**, *14*, 9065−9072.
(28) Cyriac, J.; Pradeep, T.; Kang, H.; Souda, R.; Cooks, R. G. Low-Energy Ionic Collisions at Molecular Solids. *Chem. Rev.* **2012**, *112*, 5356−5411.

DOI: 10.1021/acsami.9b00896
ACS Appl. Mater. Interfaces 2019, 11, 10237−10243